The Application of Coherent Optics to the Study of Adhesive Joints. I. Speckle Photography

M. F. VALLAT, P. MARTZ, J. FONTAINE,* and J. SCHULTZ, *Centre de Recherches sur la Physico-Chimie des Surfaces Solides, Centre National de la Recherche Scientifique, 24 Avenue du Président Kennedy, 68200 Mulhouse, France*, and *Laboratoire de Recherches sur la Physico-Chimie des Interfaces de l'Ecole Nationale Supérieure de Chimie de Mulhouse 3, Rue Alfred Werner, 68093 Mulhouse Cedex, France*

Synopsis

A new technique of coherent optics, speckle photography, has been applied to the study of the behavior of adhesive joints under shear stress. This technique allows the determination of the in-plane motion by a point-by-point analysis with a sensitivity of about 3 μm. This property has been used to measure the interfacial displacement of model glass–glass joints bonded by different types of adhesive when submitted to shear. The experimental results permit direct verification of Volkersen's theory as well as the determination of the actual shear moduli of the thin adhesive layer. The simplicity of use and interpretation of the technique of speckle photography should lead to significant application of this method in the future for the study of adhesive joints.

INTRODUCTION

The single lap shear test is one of the most common and useful techniques for studying the behavior of adhesive joints under stress. Volkersen[1] was among the first to investigate the stress distribution which is nonuniform across the lap. He calculated the stress concentrations at the ends of the lap joint. However, conventional techniques used to measure displacement or strain such as extensiometers, strain gages, or displacement transducers are not always suited to the problem. Stress analysis of lap joints have been principally investigated using the photoelastic technique,[2-5] which permits determination of local stress concentrations. Unfortunately in most cases, industrially used materials are not sufficiently birefringent, so that studies were carried out on model systems employing photoelastic materials. Extrapolation of the results using similarity criteria such as those formulated by Kutscha[6] for model rubber joints does not always permit access to the actual behavior of the joints.

Since the development of the first lasers in 1960, many new methods of measurement have appeared, and we found it interesting to investigate a new field of application for two techniques of coherent optics, namely, *speckle photography* and *holographic interferometry*. Speckle photography and holographic interferometry are complementary as the first technique is

* On leave of absence from Groupe de Recherche et d'Essais en Photonique Appliquée, 3 Rue de l'Université, 67000 Strasbourg, France.

Journal of Applied Polymer Science, Vol. 31, 309–321 (1986)
 CCC 0021-8995/86/020309-13$04.00

more sensitive to movement in the plane and the second to movement out of the plane of observation. Both techniques were used in this work. However, we will first examine the application of speckle photography to the study of the behavior of rigid joints.

Speckle photography is attractive for a variety of reasons:

—It is possible to measure, without contact and without special surface preparation, small displacements of any diffusing surface.

—An overall view of the sample behavior is obtained by a point-by-point analysis.

—The method is simple to use.

—Interpretation of the results is easy.

—All data are stored.

PRINCIPLE OF SPÈCKLE PHOTOGRAPHY

The speckle phenomenon was known as early as the last century, when it was considered as optical noise. Gabor[7] realized that it was not really noise but unwanted information. When a rough object is illuminated with laser light (highly coherent light), it was shown by different authors[8,9] that the light reflected or transmitted by this object has a granular appearance, a characteristic of the object. The phenomenon is the result of the wave nature of light and the limit of resolution of the eye lens.[10] If light reflected by the object surface is focused by a lens, the light falling on a point on the image (Fig. 1) comes from a region of the object defined by the resolving power α_R of the image lens given by[10]

$$\alpha_R = 1.22\,\lambda/D \tag{1}$$

where λ is the wavelength of the light and D is the diameter of the lens.

A point of the object corresponds to a region in the image plane and inversely a point in the image plane corresponds to a region of the object. Because laser light is highly coherent, the light scattered by one point on the object interferes with the light scattered by all other points (which are at different heights due to surface roughness). Interference results in a granular pattern of interference fringes termed speckle.

It was only with the advent of the laser that studies of this phenomenon showed how what was thought to be optical noise could be converted into

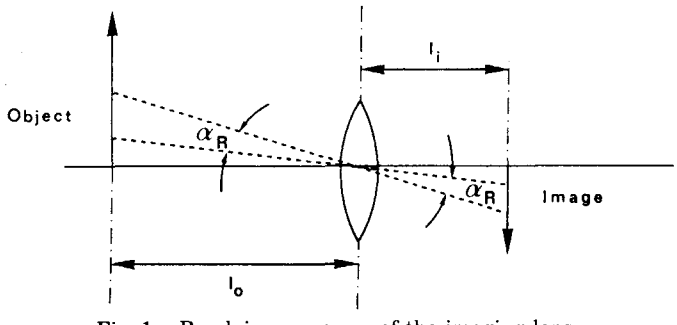

Fig. 1. Resolving power α_R of the imaging lens.

various techniques useful in metrology. During the last 12 years, the major object of speckle metrology has been the quantisation of the phenomenon.

Archbold, Burch, and Ennos[11,12] introduced speckle photography. This method is very well adapted to the measurement of displacements of a plane surface in its plane.

The specimen is illuminated by a divergent, coherent beam. The image of the surface is obtained in the imaging plane of a lens (L_2) of focal length f and diameter D (Fig. 2). The size of the speckle is small, so that the photographic emulsion on which the speckle pattern is recorded has to have an adequate resolving power.

On application of a force upon the object, two exposures, one before and one after the force is applied, are made on the same emulsion. Provided that the surface microstructure is not significantly modified, the photographic plate contains two identical speckle patterns which are only translated with respect to one another.

Coherent optical processing [Fig. 3(a)] permits measurement of the displacement of any point on the image. A narrow laser beam is made to impinge normally on a point of the recorded image. The two speckle patterns diffract the light and fringes can be observed on the screen, as shown in Figure 3(b). These patterns act as Young's slits in that they effectively split the light into two coherent sources capable of interference. The interpretation of the resultant fringes is straightforward. They are perpendicular to the displacement vector and the fringe spacing is inversely proportional to the displacement d, which is given by

$$d = \lambda L/i\Gamma \tag{2}$$

where λ is the wavelength of the light, L is the distance from the screen to the photographic plate, i is the fringe spacing, and Γ is the image-object

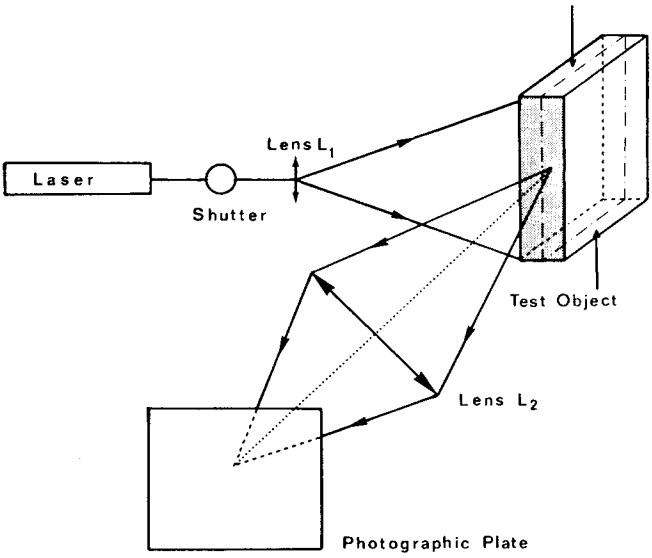

Fig. 2. Speckle photography: recording system (the test object here is the single lap shear specimen).

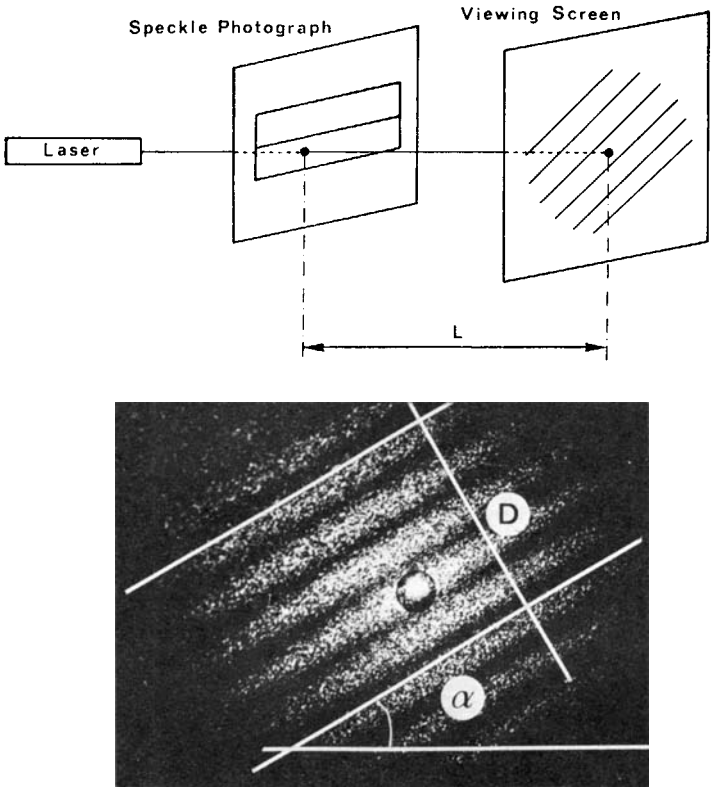

Fig. 3. Speckle photography: (a) processing system; (b) fringe pattern.

magnification. Thus a picture of the in-plane movement of the specimen surface can be constructed by a point-by-point analysis.

The smallest measurable displacement $d_{\min}$ is related to the size of the speckles and to the magnification used:

$$d_{\min} = 1.22\,\lambda(f/D)(1 + 1/\Gamma) \tag{3}$$

where f/D is the lens aperture.

Therefore, the best sensitivity will be obtained with a large aperture, i.e., low values of f/D for a given magnification. The wavelength of the helium-neon laser is 632.8×10^{-3} μm and the smallest displacement will be

$$\left.\begin{aligned}\Gamma &= 2\\ f/D &= 2.8\end{aligned}\right\} d_{\min} = 3.2\ \mu\text{m}$$

$$\left.\begin{aligned}\Gamma &= 2\\ f/D &= 1.4\end{aligned}\right\} d_{\min} = 1.6\ \mu\text{m}$$

When the displacement is too large, no correlation exists between the two patterns. In practice, the upper limit depends on the maximum number of fringes that can be counted in the diffraction halo.

However, it must be mentioned that when spurious movements or vibrations occur, aberrations will appear. Archbold and colleagues[12,13] have studied the effect of tilt and out-of-plane translation upon the resulting fringes.

EXPERIMENTAL

Materials and Testing

The test specimens are prepared with two glass plates bonded by a polymeric adhesive layer. The float glass used was neither polished nor submitted to any surface treatment. Before use, the glass plates were simply wiped with acetone and alcohol.

For a preliminary study, four adhesives were selected: an epoxy-resin (Araldite AY 103 + HY 930, Ciba-Geigy); two monocomponent and UV-curable urethane acrylic resins (Loctite 356—Loctite and NOA 65—Norland); a silicone rubber (Sylgard 184, Dow Corning).

The mechanical properties (Fig. 4) of these adhesives of 0.4–1 mm thickness were obtained from stress–strain curves at a rate of elongation of 5 mm·min^{-1}. The initial tangent modulii (Table I) corresponds to the initial slope of these curves. The conditions of curing of the adhesives are given in annex.

These results show that the adhesives depict a large range of rheological and mechanical behavior: vitreous for the epoxy resin, elastoplastic for the Loctite adhesive, and viscoelastic for the high modulus NOA 65 adhesive and the low modulus silicone rubber.

The dimensions of the glass plates are 50 × 50 × 10 mm, the thickness g of the adhesive layer ranges from a few to about 10 μm.

The cured samples were submitted to a shear test using an apparatus shown in Fig. 5.

The shear stress is applied using an antisymmetric sample holder. The sample holder is clamped to the piston of a hydraulic pump. The main

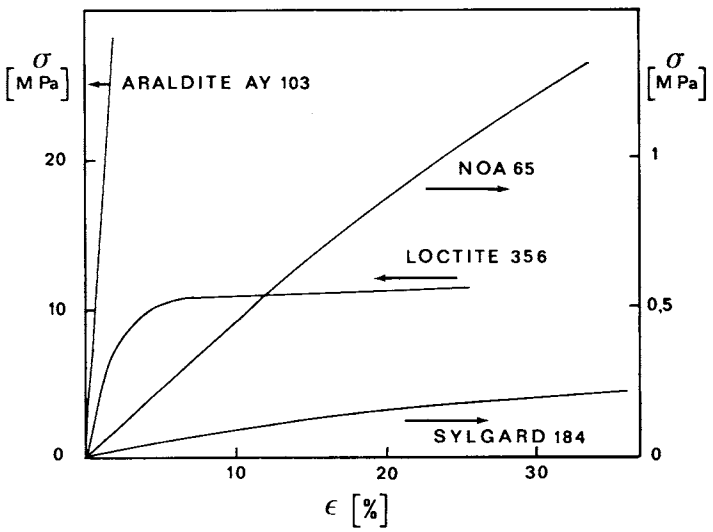

Fig. 4. Tensile stress–strain curves of the four adhesives studied.

TABLE I
Initial Tangent Moduli of the Adhesives

Adhesive	Araldite AY 103	Loctite 356	NOA 65	Sylgard 184
E (MPa)	2×10^3	5.1×10^2	4.7	1.4

advantage of this device is the absence of vibration (no disturbance of the optical experiments). The applied load was measured by means of strain gages bonded to the piston.

Application of the Speckle Photography

Two examples are given to illustrate the method. The first does not show any interfacial displacement while the second does. The specimens were observed at their edges, the reflecting power of which were increased by means of matt white paint.

The sample was illuminated by a divergent laser beam (Helium-Neon, Spectra-Physics model 124 B, 15 mW). The image of the object was focused by a photographic lens (Olympus f = 180 mm − 2,8) onto a high resolution photographic plate (Agfa Gevaert 10E75).

The exposures (a few seconds each) were made on the same photographic film. For the first one, the sample was submitted to a small load of 0.2 kN (τ = 0.08 MPa). For the second one, the applied force was set at 4.1 kN (τ = 1.6 MPa).

After development, the plate was processed as described in figure 3.a. The fringe spacing and the angle (α) of each interference pattern were determined at several points on a line normal to the joint (figure 6). The

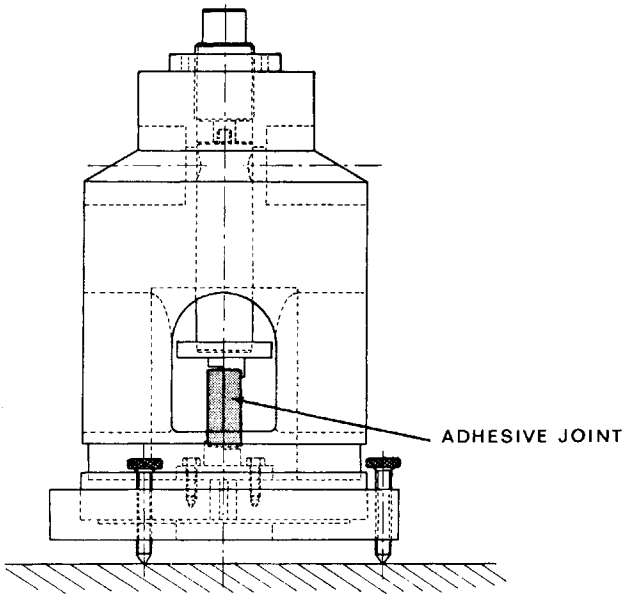

Fig. 5. Shear test apparatus.

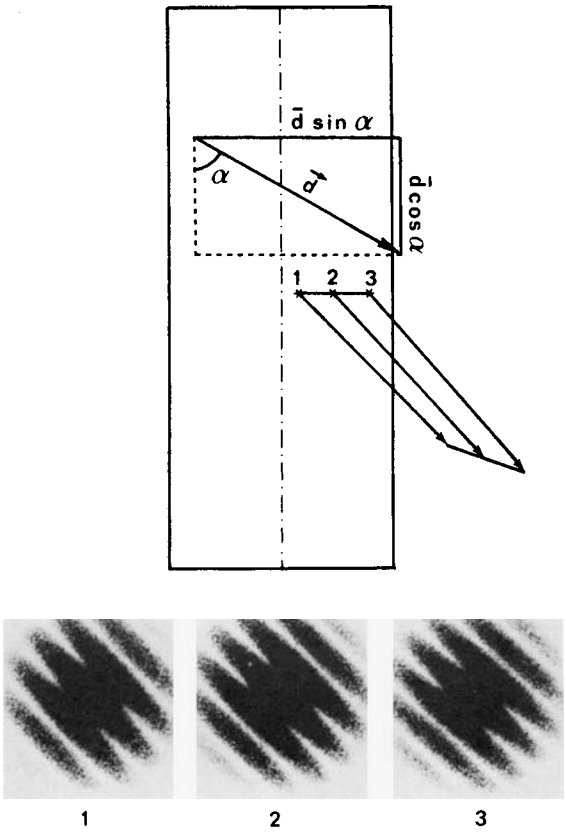

Fig. 6. Determination of the displacement vectors corresponding to three points of the edge surface of the test sample.

displacement was calculated (equation 2), thus yielding the displacement vector ($\vec{d}$) for each point investigated. Such measurements were made on the whole of the image, so that movement of the specimen could be determined.

Figure 7 is relative to the first example with no interfacial displacement. The dotted lines between the image points examined (initial gratings) correspond to the initial state. Because of the small size of the displacements occuring at each point we had to use different scales to plot the measured displacement and the initial sample state. The grating joining the displacement vectors is drawn in solid lines and can be superimposed on to the initial grating.

As a consequence, within the limits of sensitivity of the method, the sample did not undergo any detectable deformation. Moreover, the grating being continuous through the interface, there is no interfacial displacement. The in-plane movement is thus a whole motion resulting from the combination of a translation and a rotation. The center of rotation cannot be determined; however, an angle of rotation β can be defined. The observed tilt could originate from the torque exerted, from the running clearance between the piston and the bore and/or from diverse mechanical imperfections in either the samples or the apparatus. It is worth noting that this

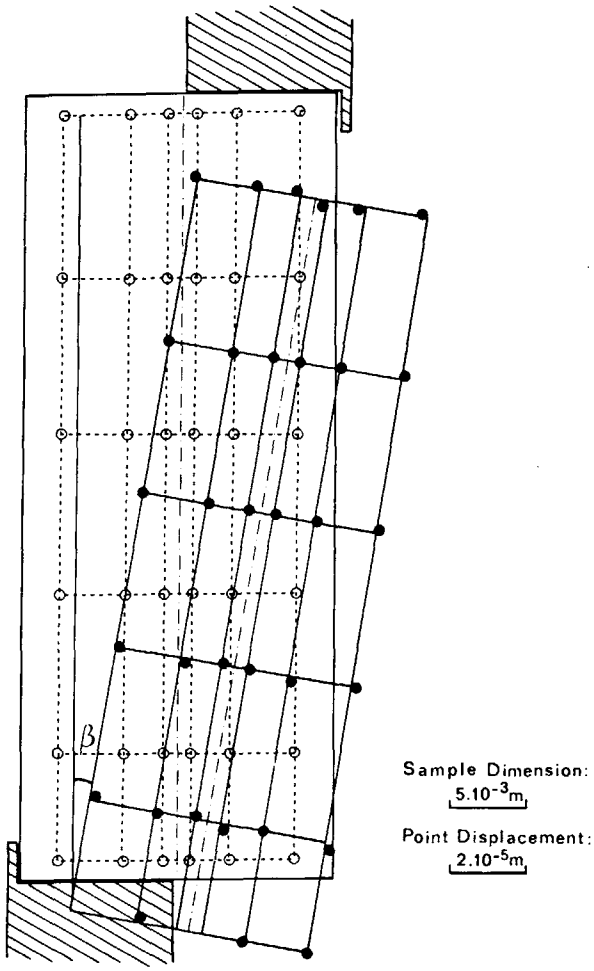

Fig. 7. Point-by-point analysis of a sample with no interfacial displacement.

angle is always small. In this example, β is equal to 4×10^{-2} degree. In all cases, β is lower than 0.1°. This value proves, on the one hand, the high sensitivity of the method and, on the other, the good stability of the apparatus.

The second example showing an interfacial displacement is given in Figure 8. In this case, it is impossible to draw a single grating which will traverse the interface. The grating is divided into two parts: one for each glass plate. The distance separating the points before and after the force was applied are the same. Consequently, as before, within the limits of sensitivity, the glass is not deformed. The two plates are moving in opposite directions. This shift results from the strain of the adhesive in the field of forces considered. As in the first example, it is possible to define a tilt which, in this case, is equal to 0.03°.

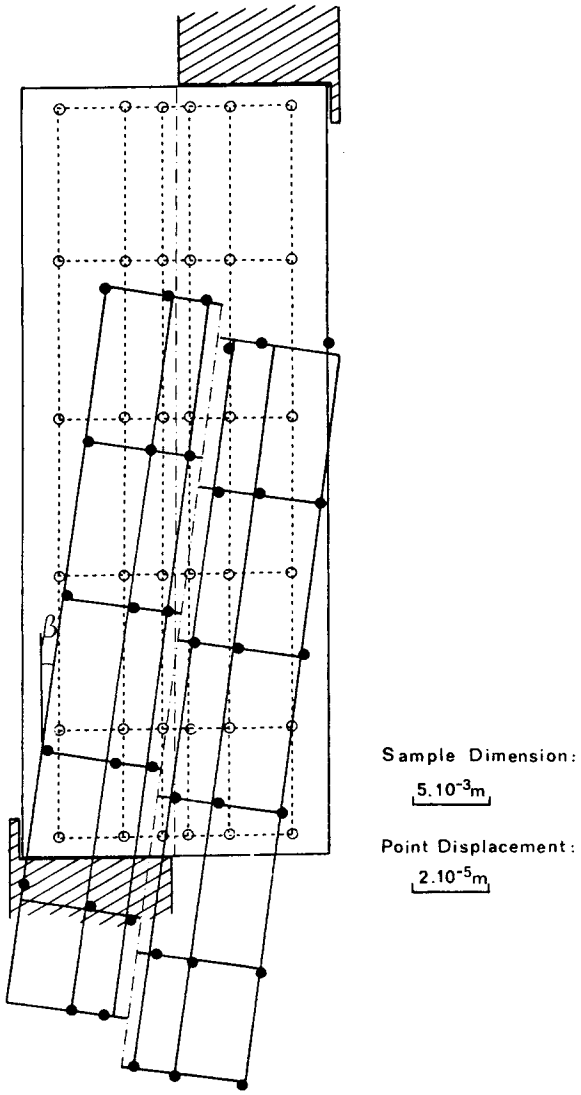

Fig. 8. Point-by-point analysis of a sample with an interfacial displacement.

RESULTS AND DISCUSSION

The stresses in a lap joint under tensile or compressive load are representative of those met in the joints between rigid bodies. Generally, the adhesive layer is subjected to a combination of shear and normal stresses. Before inception of the adhesive joint, the stress distribution was often studied because assemblies (usually joints between metals) were bolted, riveted, or welded.

A general review of properties of glass–glass joints is given by Dumig and Schaudel.[14] In particular, theoretical analysis of the stress distribution may be considered as a simple case of metallic lap joints because the sub-

strate behaves as an ideal elastic material. Here, the simplest analysis developed by Volkersen[1] was used. The deformation of the adhesive layer is given by the expression:

$$\delta(x) = \frac{-Fqg}{4Gc\omega}\left(\sinh qx + \frac{\sinh q \cosh qx}{1 - \cosh q}\right) \tag{4}$$

with

$$q = \left(\frac{8\,G}{E\,g\,h}\right)^{1/2} c$$

G is the shear modulus of the adhesive, and E is the Young's modulus of the glass. The other parameters are given in Figure 9.

Thus, for the four adhesive joints studied, we have calculated the values of the deformation δ according to Volkersen's theory. We will subsequently compare these values with those obtained by speckle photography.

The first example given in which there is no interfacial displacement is representative of joints obtained with the high modulus resins (Araldite and Loctite) when the applied force is less or equal to 5 kN ($\tau \leqslant 2$ MPa). In Figure 10, the calculated deformations along the interface for these two adhesives are reported for two different thicknesses ($g = 10$ and 30 μm) and for an applied force of 5 kN. It is interesting to note that the calculated deformations are very small for both adhesives ($\leqslant 1$ μm). Accordingly, no

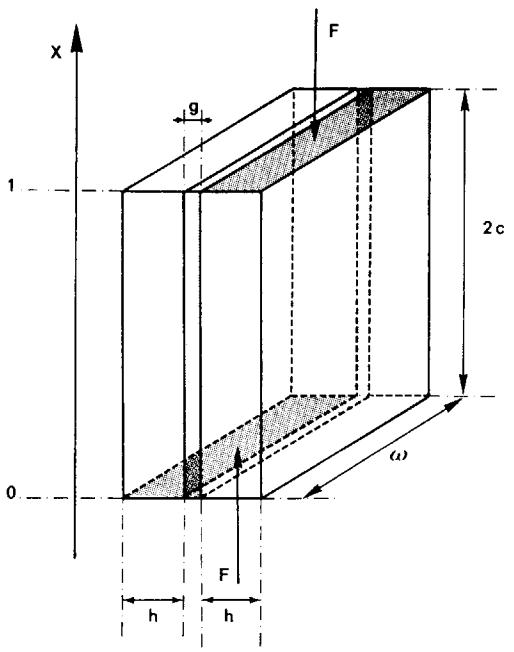

Fig. 9. Description of the test samples. In this case $\omega = 2c = 5 \times 10^{-2}$ m, $h = 10^{-2}$ m, $10^{-5} \leqslant g \leqslant 3 \times 10^{-5}$ m.

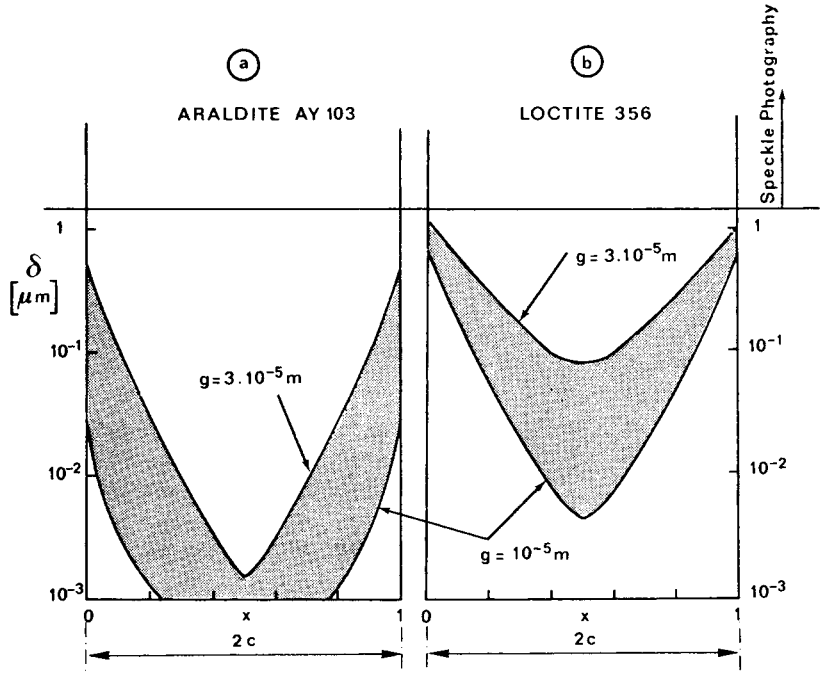

Fig. 10. Deformation of the adhesive layer along the interface calculated according to Volkersen: (a) for Araldite; (b) for Loctite.

displacements were measured experimentally. However, it should be noted that the sensitivity of holographic interferometry is sufficient to detect these interfacial displacements at the ends of the joints in the case of Loctite.

The second example is typical of joints obtained with NOA resin. In this case, the displacement is measurable and homogeneous along the overlap. The calculated deformation is plotted in Figure 11 for an applied force of 5 kN.

If the adhesive thickness is made equal to 15 μm, the corresponding calculated deformation is 19.7 μm at the ends of the joint and 18 μm in the middle. The difference (1.7 μm) between the two values is of the same order as the experimental error. Experimental results obtained by speckle photography are in good agreement with the theory ($\delta \simeq 20$ μm) as shown below.

For a gradually applied stress, the deformation can be determined at each stage. It is nevertheless necessary to check that the adhesive does not creep. Thus, δ_c the cumulative deformation is given by

$$\delta_c = \sum_{i=1}^{n} \delta_n$$

where n is the number of stages.

In Figure 12, δ_c is plotted as a function of the applied force. The apparent shear modulus can be determined using these experimental results. For an adhesive joint of 15 μm thickness, we obtain a value of 1.6 MPa, which is in good agreement with the value determined directly using thick films.

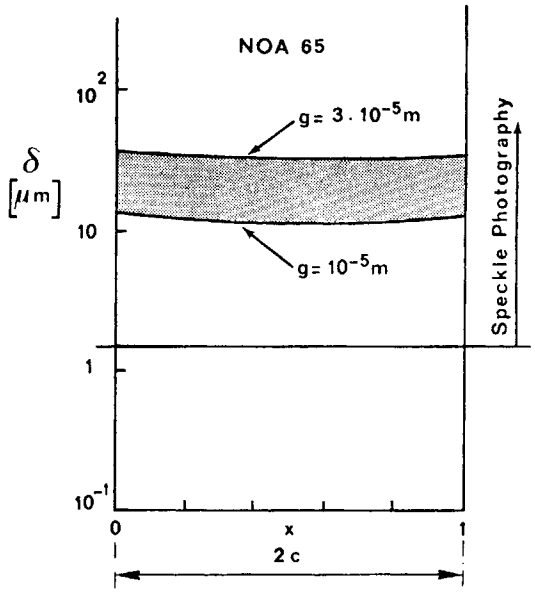

Fig. 11. Calculated deformation along the interface for NOA 65 adhesive.

Therefore, the measurement of adhesive deformation by speckle photography permits verification of Volkersen's theory, direct determination of the shear stress–strain curves and gives access to the adhesive shear modulus.

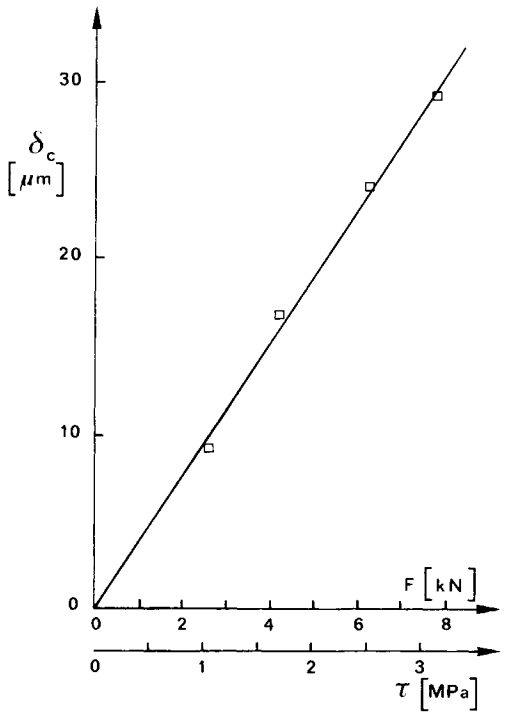

Fig. 12. Interfacial displacement versus applied force F or shear stress τ.

Under our experimental conditions, the silicone adhesive could not be studied. Even by only slightly increasing the applied force between stages, it was not possible to obtain any information due to adhesive creep. Therefore, the exposure times are too long. However, it would be possible to study such adhesives by using a much more powerful laser which would require shorter exposures.

CONCLUSION

We have applied speckle photography to the study of rigid joints under shear stress. The in-plane motion of the sample leading to interfacial displacement was determined; this displacement corresponds to the adhesive strain in the field of forces considered. The experimental results permitted direct verification of Volkersen's theory in the case of glass–glass joints and determination of the shear stress–strain curve. Knowing this curve, the adhesive modulus can be calculated. Therefore, using the proposed method, we can directly obtain the shear modulus of thin films. This result is very important in that the influence of the substrate on the properties of this polymeric films may be demonstrated.

The technique of speckle photography is relatively easy to employ and constitutes a useful tool for the study of the behavior of all kinds of rigid adhesive joints.

APPENDIX: CONDITIONS OF CURING

Araldite AY 103 and Hardener HY 930. 10 parts by weight of hardener are added to 100 parts of resin. The mixture is cured at 28°C during 21 h.

NOA 65 and Loctite 356. The resins are exposed to ultraviolet light (Philips HPK 125 W lamp) during 10 min. The lamp is placed at a distance of 180 mm of the film. A glass plate of 10 mm thickness is interposed between the adhesive film and the lamp.

Sylgard 184. One part by weight of catalyst is mixed with 10 parts of resin. The mixture is cured at 60°C during 5 h.

The authors acknowledge with thanks the help of Mr. J. Fatkin in preparing this manuscript.

References

1. O. Volkersen, *Luftfahrforsch.*, **15**, 41 (1938).
2. C. Mylonas, *Proc. 8th Int. Congr. Appl. Mech.*, **4**, 137 (1948).
3. C. Mylonas, *Proc. Soc. Exper. Stress Anal.* **XII**(2), 129 (1955).
4. A. S. MacLaren and I. MacInnes, *Br. J. Appl. Phys.*, **9**, 72 (1958).
5. E. Sancaktar and P. O. Lawry, *J. Adhesion*, **11**, 233 (1980).
6. D. Kutscha, U. S. Forest Products Laboratory, Technical Report MLTDR-64-298, (1964).
7. D. Gabor, *Proc. Soc. Photo-Opt. Instrum. Eng.*, **25**, 129 (1971).
8. J. D. Rigden and E. I. Gordon, *Proc. Inst. Radio Eng.*, **50**, 2367 (1962).
9. B. M. Oliver, *Proc. Inst. Electrical Electron. Eng.*, **51**, 220 (1963).
10. R. R. Hudson and D. P. Setopoulos, *Strain*, **11**, 126 (1975).
11. E. Archbold, J. M. Burch, and A. E. Ennos, *Opt. Acta*, **17**, 833 (1970).
12. E. Archbold and A. E. Ennos, *Opt. Acta*, **19**(4), 253 (1972).
13. E. Archbold, A. E. Ennos, and M. S. Virdee, *Soc. Photo-Opt. Instrum. Eng., 1st Eur. Congr. Opt. Appl. Metrol.*, **136**, 258 (1977).
14. W. Dumig and D. E. Schaudel, *Adhäsion*, **1**(3), 70 (1978); **2**(4), 107 (1978); **3**(5), 145 (1978); **4**(8), 252 (1978); **5**(9), 288 (1978).

Received March 6, 1984
Accepted November 30, 1984